JOURNAL OF VIROLOGY, Oct. 1971, p. 534-550
Vol. 8, No. 4

Mechanism of Intranuclear Crystal Formation of Herpes Simplex Virus as Revealed by the Negative Staining of Thin Sections

KANEATSU MIYAMOTO
Flow Laboratories, Inc., Rockville, Maryland 20852

Received for publication 4 June 1971

Structural alterations induced in HeLa cells by herpes simplex virus and the mechanism whereby the virus is formed in the nucleus in crystal arrays were studied by electron microscopy with both the usual and negatively stained sections. Aggregates of granular and filamentous material were observed in the cytoplasm of infected cells with both sections. On the other hand, no remarkable alterations in appearance of the cytoplasmic ground substance were observed with the usual sections of infected cells. However, the cytoplasmic ground substance of infected cells when negatively stained consisted of granular material which was different in appearance from the spongy material constituting the cytoplasmic matrix of uninfected cells. In the nucleus of infected cells, complexes consisting of round bodies, amorphous material, aggregates of uniform granules in rows, and viral crystals were often observed near the nuclear membrane in both types of sections. Examinations of the granular aggregates with negatively stained sections suggested that each granule represents a subunit and that the several adjoining subunits (approximately eight) constitute the requirement for formation of a single viral capsid with a core. Thus, rapid and simultaneous formation of the core and capsid within the aggregate would replace the rows of the granules with the viral crystal. The advantages of negative staining of thin sections for visualization of fine structural alterations are discussed.

Electron microscopic studies with thin sections have revealed ultrastructural alterations induced in host cells by virus infection. In such studies, however, a question may be raised as to whether all structures induced in cells can be visualized in the thin sections. It is not a warranted assumption that the heavy metals usually employed for staining of thin sections can bind entirely and differentially to the material constituting each cellular component. Therefore, it would appear likely that some fine cellular structures might be lost to view partially or totally in the usual type of thin sections. On the other hand, it is evident that the negative-staining technique (4) usually employed for specimens unembedded in plastics, such as purified virus, is useful to resolve surface detail by outlining or embedding it with electron-dense stains. Thus, it would be expected that the application of the negative-staining technique to thin sections may provide a better tool to visualize the entirety of each cellular component and to obtain detailed information concerning morphogenetic events in infected cells.

Although the mechanism of herpes virus replication in the nucleus has not been determined, cells infected with herpes simplex virus (HSV) have been studied by many investigators with the usual thin sections (2, 5, 9, 13, 15, 19-21, 23), and the manner in which the viral particles are formed has been reported. Furthermore, localization in infected cells of viral antigens associated with and without viral particles has been demonstrated by use of ferritin-conjugated antibodies specific for HSV (7, 14). By the use of such an extensively studied virus, an attempt was made in the present study to re-examine HSV-infected cells with the negatively stained sections in comparison with the observations by the usual thin sections. Cells for negative staining were dried after usual fixation and dehydration procedures and were then embedded into epoxy resin in the usual manner. The thin sections were stained with phosphotungustic acid (PTA).

The results reported here indicate that the fine structural alterations induced in cells by HSV infection can be visualized in detail in negatively stained sections.

MATERIALS AND METHODS

Cells and culture media. Monolayer cultures of HeLa cells were grown in Eagle's minimal essential medium (MEM) supplemented with 10% fetal calf

serum (FCS). After infection, the cells were maintained with MEM supplemented with 5% FCS.

Virus. The Miyama strain (12) of HSV, kindly provided by Councilman Morgan, Columbia University, New York, was used.

Fixation and embedding. Uninfected HeLa cells and cells infected with a high multiplicity (approximately 10 $TCID_{50}$ per cell) of the virus at 37 C for 17 hr were washed twice with Earle's solution, fixed in situ for 30 min at 4 C with 1% glutaraldehyde in Sorenson's phosphate buffer (*p*H 7.2), washed thoroughly with Earle's solution in situ, scraped, and pelleted. The cell pellet was fixed for 30 min at 4 C with 1% osmium tetroxide in phosphate buffer (6), washed with Earle's solution, and dehydrated with graded ethanol in a usual manner. After completion of dehydration with absolute ethanol, the cell pellet was cut into two pieces in ethanol. One piece of the cell pellet was immediately treated with propylene oxide and embedded into epoxy resin (Epon 812) in the usual manner. The other piece of the pellet was transferred onto a filter paper, put into a desiccator with phosphorous pentoxide (P_2O_5), and dried for 3 to 17 hr at room temperature. The dried cell pellet was immersed into absolute ethanol twice. This procedure was done in an evacuated desiccator (less than 20 mm of Hg) to eliminate air from, and to accelerate penetration of ethanol into, the dried cell pellet. Elimination of air could be seen as tiny bubblings from the pellet. This cell pellet was then treated with propylene oxide twice and embedded into epoxy resin in the usual manner.

Electron microscopy. The thin sections of the cells prepared in the usual manner were stained with uranyl acetate followed by lead citrate (18). The thin sections of the cells dried prior to embedding were stained with 2% PTA (aqueous solution adjusted to *p*H 6.5 with KOH) as follows; copper grids were floated, section side down, on the stain and removed after 30 to 60 min. Excess stain was removed with filter paper and the sections were dried in the air without washing. These sections were examined in an Hitachi HU-11E electron microscope.

RESULTS

Figures 1 and 2 illustrate parts of the cytoplasm and nuclei (at the right) of uninfected HeLa cells. In Fig. 1, cells were prepared for electron microscopy in the usual manner, the thin sections of which were stained with uranyl acetate and lead citrate. The nuclear membrane, mitochondrion, and Golgi area are stained positively and many ribosomes are seen scattered throughout the cytoplasm. Such thin sections will be referred to hereafter as the "usual" sections. In Fig. 2, however, cells were dried after usual fixation and dehydration and then embedded into epoxy resin, the thin sections of which were stained with PTA. The nuclear membrane, mitochondria, and a well-developed Golgi area show negative contrast although ribosomes seen in Fig. 1 are not discernible. Such thin sections will be referred to hereafter as the "negatively stained" sections.

Figures 3 to 5 show parts of the cytoplasm and nuclei of uninfected HeLa cells at high magnification. In the usual sections (Fig. 3), the cytoplasmic matrix (at the right) consists of amorphous material of low density. Ribosomes are scattered throughout the cytoplasm, some of which are attached to the membrane of the endoplasmic reticulum. The nuclear matrix (at the left) appears to consist of granular and filamentous material. In the negatively stained sections (Figs. 4 and 5), however, the cytoplasmic matrix as well as the mitochondrial matrix in Fig. 4 appear to be packed with spongy material, and no ribosomes are discernible in the cytoplasm, as noted in Fig. 2. The nuclear matrix (Fig 5) also appears to be filled with spongy material. The lumen of the endoplasmic reticulum seen in both sections (Fig. 3 and arrows in Fig. 4) contains finely granular material.

Figures 6 to 8 illustrate parts of the cytoplasm of HSV-infected HeLa cells and enveloped virus particles on the cell membrane. In the usual sections, as shown in Fig. 6, the cytoplasmic matrix of infected cells does not appear to differ from that of uninfected cells in the appearance of the cytoplasmic ground substance and in the distribution of ribosomes (cf. Fig. 6 with Fig. 1 and 3), except for the presence of viral capsids with dense cores (at the extreme right) free in the cytoplasm. When the thin sections, taken from the same block as Fig. 6, were stained with PTA in the same manner as for the negatively stained sections, cellular structures and viruses appeared to be stained positively but with low contrast and were similar in appearance to those in Fig. 6. In the negatively stained sections, however, the cytoplasmic matrix of infected cells consists of granular material, (Fig. 7). Such cytoplasmic ground substance is different in appearance from that of uninfected cells (cf. Fig. 7 with Fig. 2 and 4). The viral envelope in the usual sections (Fig. 6) shows a clear limited membrane, whereas in the negatively-stained sections (Fig. 7) the envelope appears to consist of only an amorphous material without the limited membrane. The relatively electron-translucent material surrounded by the viral capsid free in the cytoplasm and in the enveloped particles seen in the negatively stained sections (Fig. 7) corresponds to the dense viral core, such as shown in Fig. 6, since in the usual sections more than 99% of enveloped particles contained dense cores. In Fig. 8, the thin sections, taken from the same block as Fig. 7, were stained with uranyl acetate and lead citrate instead of PTA, in the same manner as the usual sections. The granularity of the cytoplasmic matrix visualized in Fig. 7 is not discernible. Some ribosomes appear to be stained positively, but the cellular membranes are clearly stained negatively.

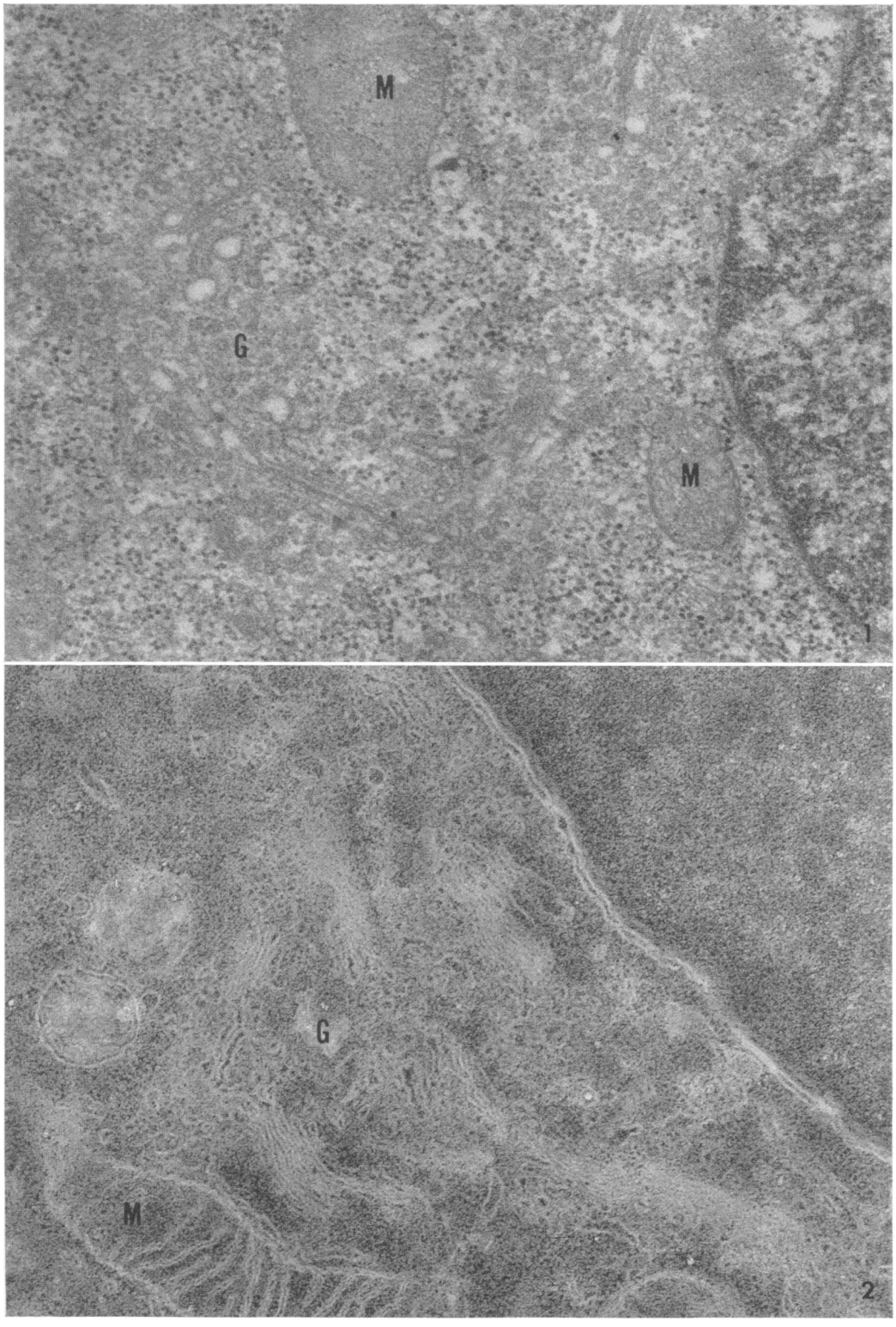

FIG. 1 and 2. *Parts of the cytoplasm and nuclei (at the right) of uninfected HeLa cells. M, mitochondria; G, Goli area.* FIG. 1. *Usual sections.* × *50,000.* FIG. 2. *Negatively stained sections.* × *50,000.*

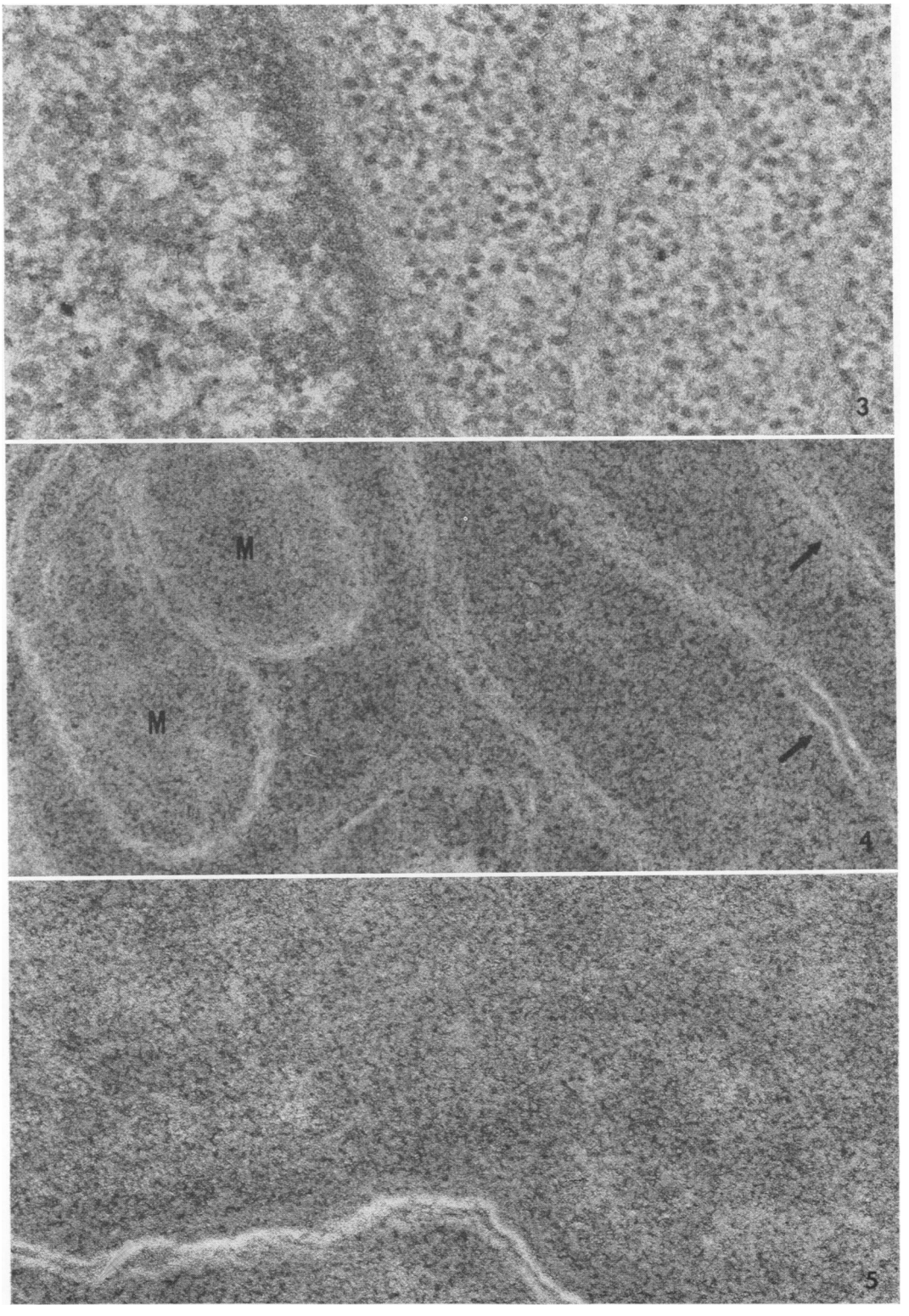

FIG. 3–5. *Parts of uninfected HeLa cells at high magnification.* FIG. 3. *Cytoplasmic matrix (at the right) and nuclear matrix (at the left). Usual sections.* × *105,000.* FIG. 4. *Cytoplasmic matrix packed with spongy material. Ribosomes are not discernible. Arrows, endoplasmic reticulum; M, mitochondria. Negatively stained sections.* × *105,000.* FIG. 5. *Nuclear matrix filled with spongy material. Part of the nuclear membrane is seen at the extreme lower left. Negatively stained sections.* × *115,000.*

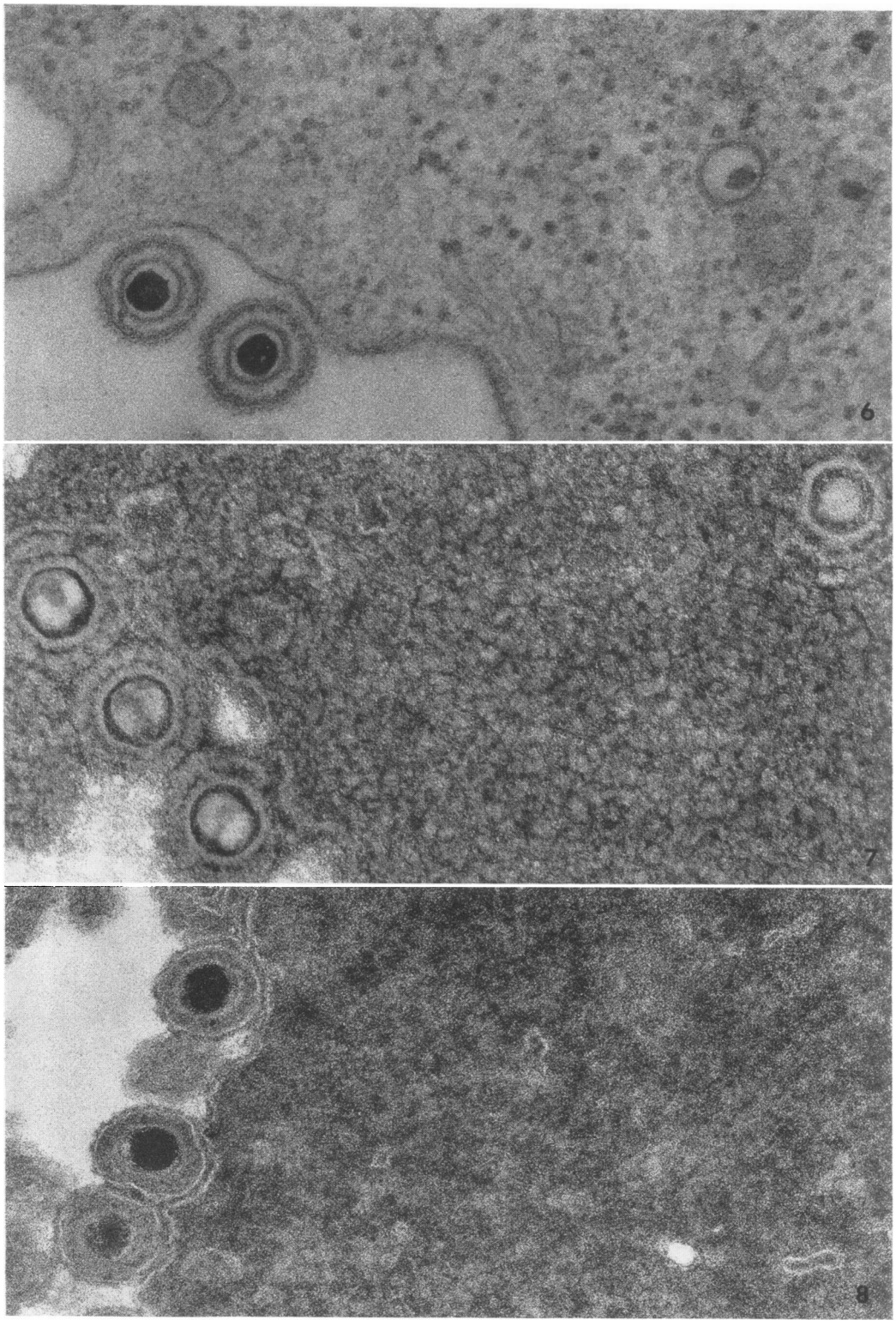

FIG. 6–8. *Parts of the cytoplasm of HSV-infected HeLa cells and enveloped virus particles on the cell membrane.* FIG. 6. *Usual sections.* × *105,000.* FIG. 7. *Cytoplasmic matrix consisting of granular material. Negatively stained sections.* × *115,000.* FIG. 8. *Thin sections, taken from the same block as Fig. 7, were stained with uranyl acetate and lead citrate, instead of phosphotungstic acid. Note positive staining of the viral core and negative staining of the membranes.* × *105,000.*

The viral core appears to be stained positively, whereas the capsid and the limited membrane of the envelope are stained negatively (these points will be discussed later).

Figures 9 and 10 show aggregates of granular and filamentous material which were observed in the cytoplasm of HSV-infected HeLa cells but not in uninfected cells. Such aggregates were encountered both in the usual (Fig. 9) and the negatively stained sections (Fig. 10) and were frequently localized near the cell membrane (Fig. 9) or near the nucleus (Fig. 10). Note in Fig. 10 that the cytoplasmic matrix consists of granular material, similar to that noted in Fig. 7 (also see Fig. 11).

The following micrographs (Fig. 11–22) illustrate parts of nuclei of HSV-infected HeLa cells. Figure 11 (negatively stained sections) shows three round bodies of different size, which are localized in the nucleus near the nuclear membrane (at the extreme left). The surface of the upper two round bodies appears smooth, whereas the surface of the other round body appears irregular and is covered with amorphous material of different density. Such round bodies did not appear to be associated with the nucleolus. The nuclear matrix consists of granular material of various size. The inset of Fig. 11 illustrates a dense round body seen in the usual sections.

Figure 12 (negatively stained sections) shows an intranuclear complex which consists of a round body, an aggregate of amorphous material (arrow), an aggregate of granules, and rows of virus. The granules appear to be relatively uniform in size and shape and arranged relatively regularly in rows. A nuclear complex in the usual sections, similar to that in Fig. 12, is shown in Fig. 13, where a dense body appears to be disintegrating and the resulting amorphous material has protruded into a collection of granules in rows, some of which have an electron-translucent center. Some granules are also seen within the viral crystal at its upper right portion where the rows of capsids are disconnected. Partially formed viruses (arrows) are localized at the peripheral portions of the crystal and within the collection of granules.

Figures 14 and 15 (negatively stained sections) illustrate two granular aggregates in different nuclei which have been sectioned at a slightly different level. In both micrographs, capsids with cores, some of which are presumably in the process of formation, are scattered within the aggregates (arrows). In insets A and B of Fig. 15, parts of granular aggregates are shown at high magnification. Although each of the granules in the negatively stained sections (inset A) appears to be arranged more closely than those in the usual sections (inset B), the center-to-center distance between two adjoining granules in a row is approximately 48 nm in both sections. The granules in the negatively stained sections (inset A) are approximately 40 nm in diameter, whereas those in the usual sections (inset B) are 35 nm. Figure 16 (usual sections) illustrates viruses at various stages of formation within a granular aggregate. Some cores partially enclosed by the capsid (arrows) appear to consist of granular material. Figure 17 (negatively stained sections) shows an area similar to Fig. 16. Here, some capsids partially formed (arrows and a crossed arrow) apparently enclose three to four granules. Such granules are similar in appearance to the granules which themselves constitute the aggregate. Furthermore, the granular core partially enclosed by the capsid (crossed arrow) at the peripheral portion of the viral crystal appears similar in its diameter to the outside length of the two adjoining granules which are localized at the immediate upper left of the granular core. Capsids in both sections are approximately 85 to 90 nm in inside diameter and 95 to 100 nm in outside diameter. Figure 18 (negatively stained sections) illustrates viral cores and capsids in various stages of formation within a granular aggregate adjacent to a round body (at the lower left), whose surface is covered with amorphous material, similar to that noted in Fig. 11 and 12. The majority of the cores fully or partially enclosed by the capsid show doughnut shape (also see Fig. 13, 16, and 17). Figure 19 (negatively stained sections) shows a viral crystal. The granules are not seen within the crystal, but some are localized at the peripheral portion of the crystal (at the upper left). The majority of the cores do not show either granularity or doughnut shape. Such viral cores are presumably those of low density since, in the usual sections (see Fig. 13), the majority of the capsids constituting the crystal contained cores of low density at 17 hr after infection. However, few capsids (arrows) contain dense cores (cf. Fig. 19 with Fig. 7). The very electron-translucent areas in the portion surrounded by the capsids represent artifacts resulting from the difficulty in penetration of epoxy resin into dried capsids (also see Fig. 12 and 20).

Figure 20 (negatively stained sections) may illustrate an advanced stage of events occurring in such a nuclear complex as shown in Fig. 12. The upper half portion of a round body near the nuclear membrane (at the lower left) has been extensively disintegrated, and the resulting amorphous material appears to be localized in the area between a viral crystal and the round body. Small aggregates of granules are seen adjacent

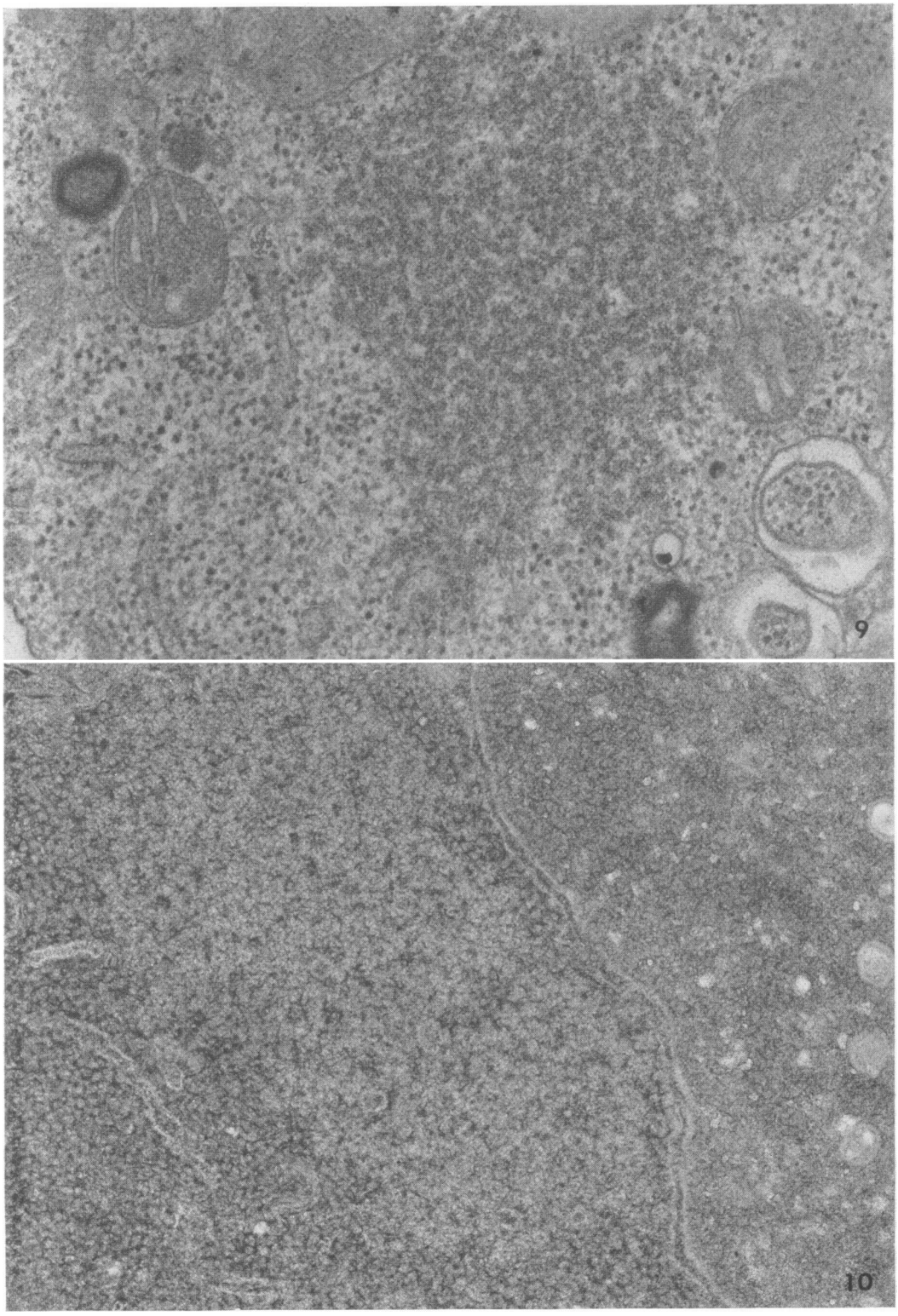

FIG. 9 and 10. *Aggregates of granular and filamentous material in the cytoplasm of HSV-infected HeLa cells.* FIG. 9. *Usual sections.* × *62,500.* FIG. 10. *Part of a nucleus with capsids is shown at the right. Note the cytoplasmic ground substance consisting of granular material, similar to that shown in Fig 7. Negatively stained sections.* × *62,500.*

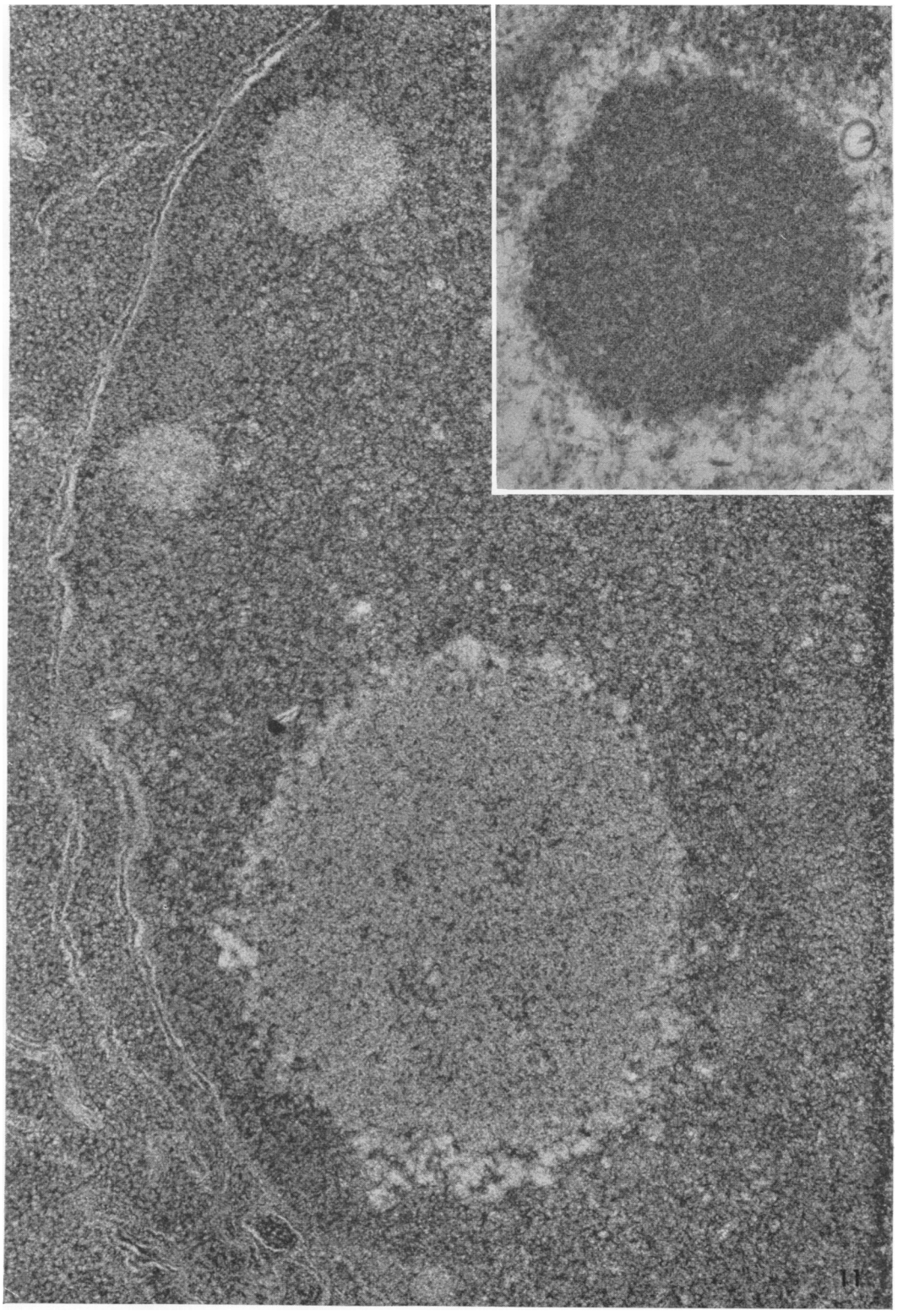

FIG. 11. *Three round bodies in a nucleus of HSV-infected HeLa cells. Negatively stained sections.* × *48,000. The inset shows a similar nuclear dense body near the nuclear membrane (at the upper left) seen in the usual sections.* × *62,500.*

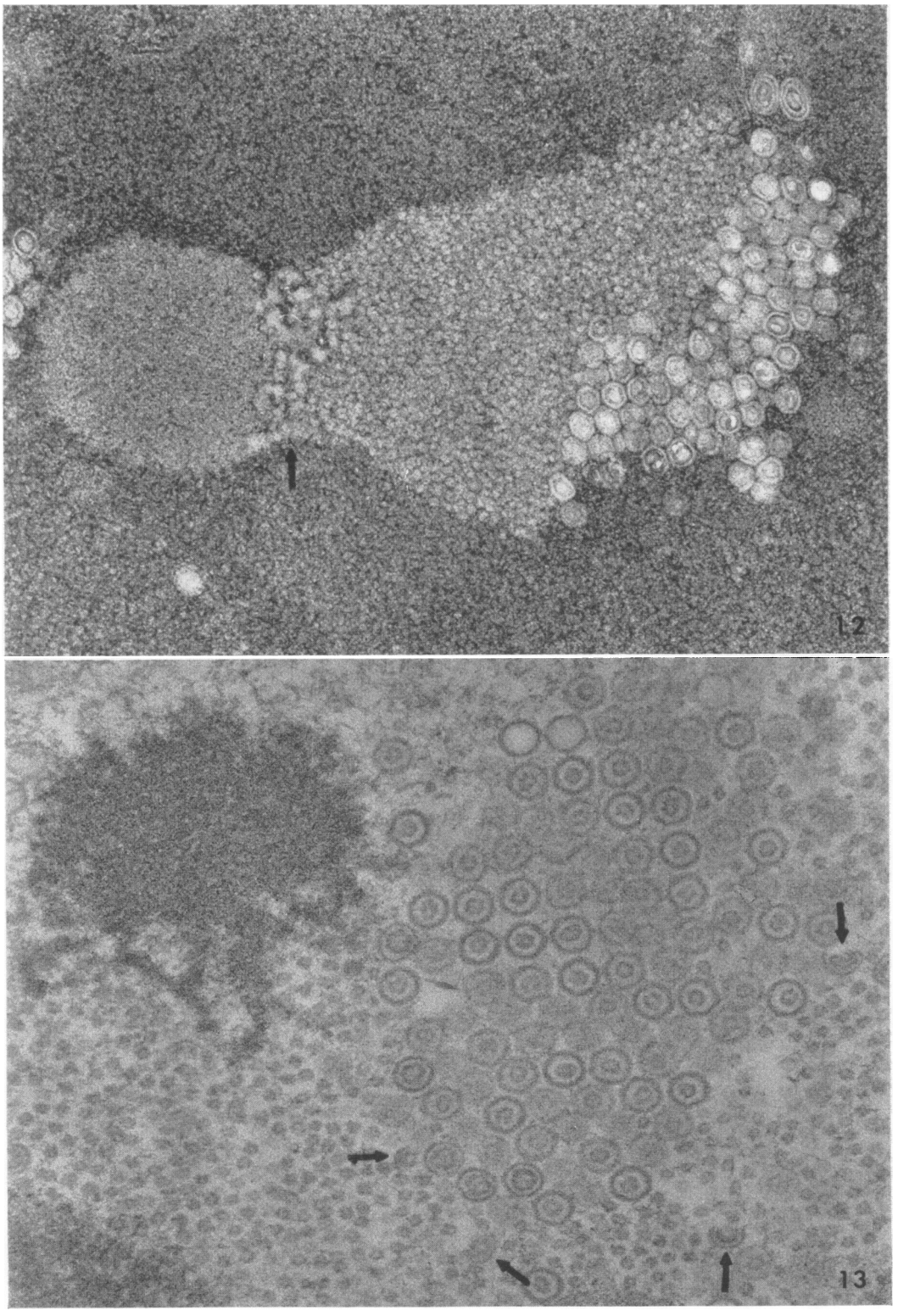

FIG. 12. *Nuclear complex consisting of a round body, amorphous material (arrow), an aggregate of uniform granules, and rows of virus. Negatively stained sections.* × *40,000.*

FIG. 13. *Nuclear complex similar to Fig. 12. A dense body is disintegrating. Partially formed viruses (arrows) are seen within the granular aggregate. Usual sections.* × *62,500.*

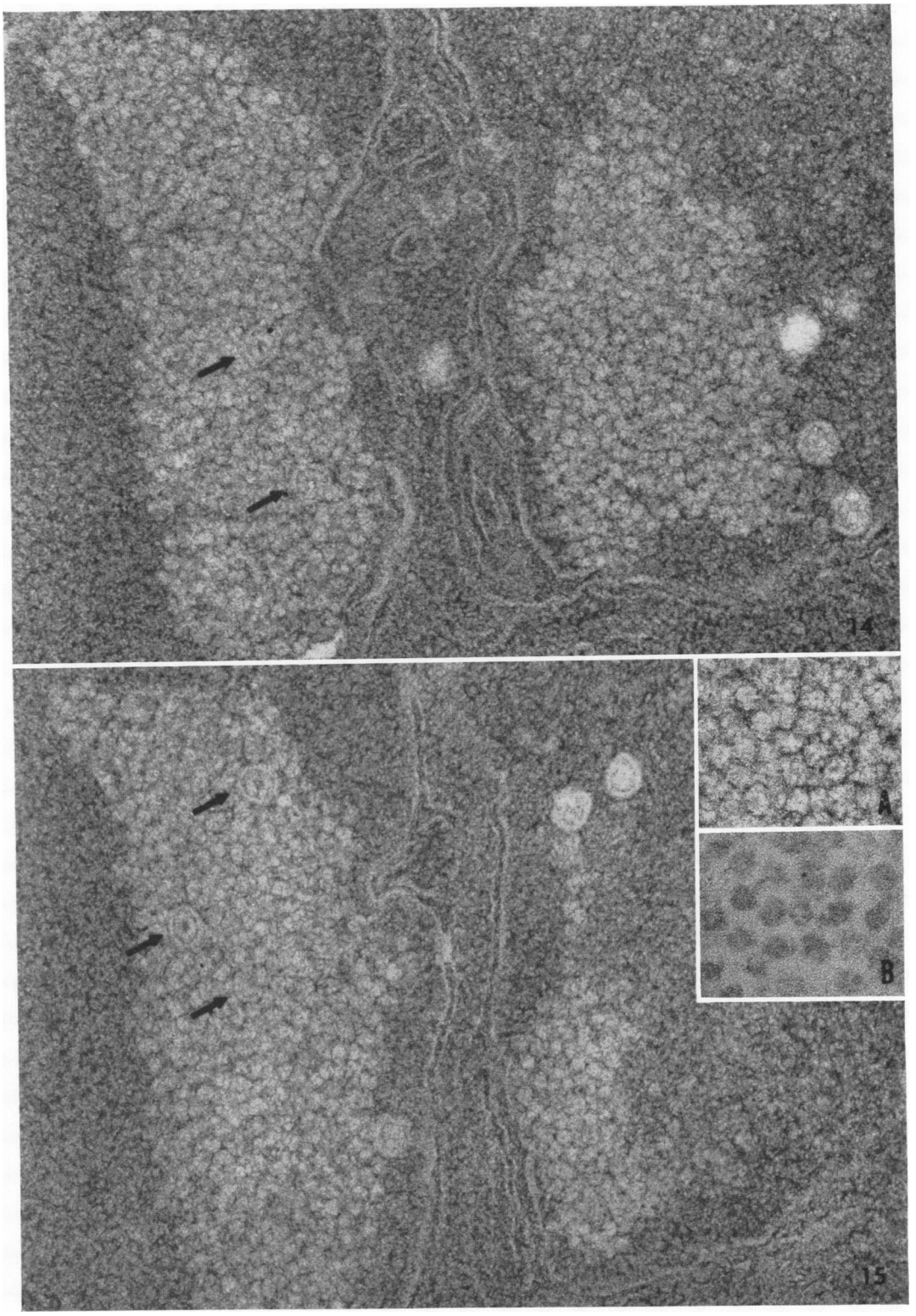

FIG. 14 and 15. *Two granular aggregates in different nuclei which have been sectioned at a slightly different level. Capsids are seen within the aggregates (arrows). Negatively stained sections. Both micrographs* × *62,500. The insets of Fig. 15 show at high magnification parts of granular aggregates seen in the negatively stained (A) and usual sections (B). Both micrographs.* × *105,000.*

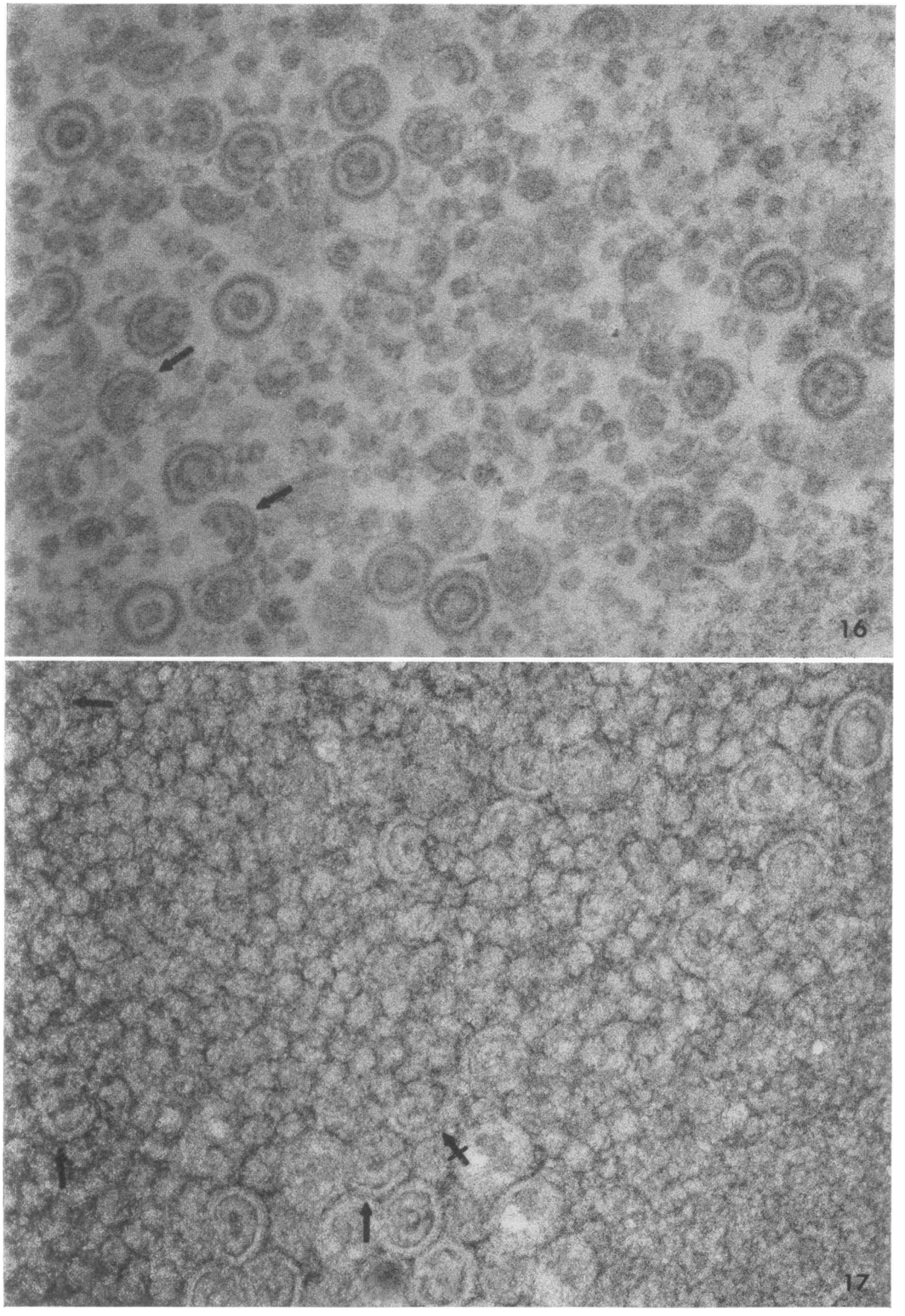

FIG. 16 and 17. *Viruses at various stages of formation within granular aggregates.* FIG. 16. *Some capsids partially formed (arrows) appear to enclose granular material. Usual sections.* × *105,000.* FIG. 17. *Some capsids partially formed (arrows and a crossed arrow) enclose several granules. Negatively stained sections.* × *105,000.*

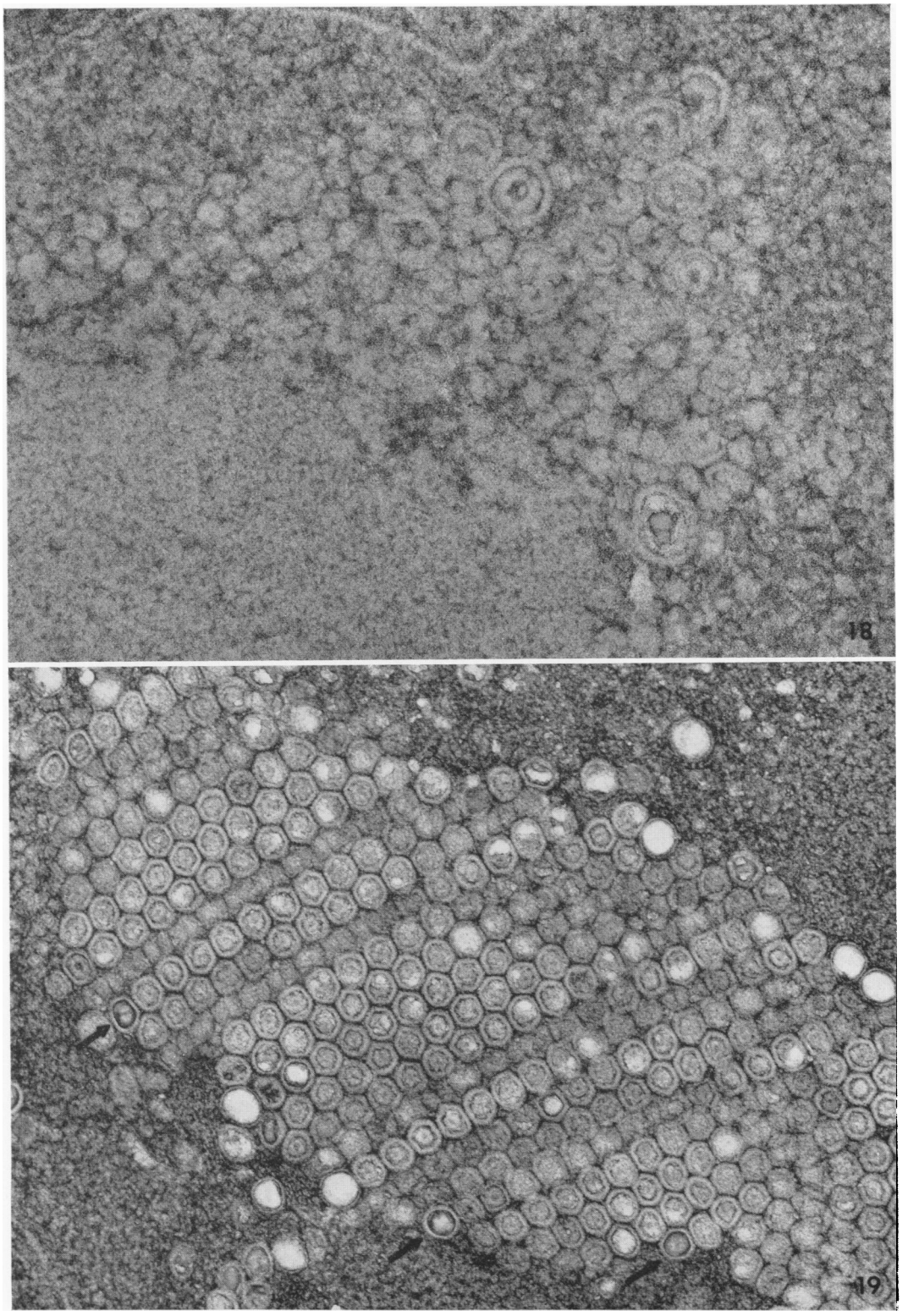

FIG. 18. *Viruses within a granular aggregate adjacent to a round body (at the lower left). The majority of the cores partially or fully enclosed by the capsid show doughnut shape. Negatively stained sections.* × *105,000.*

FIG. 19. *Viral crystal in the negatively stained sections. The majority of capsids contain cores of low density but some (arrows) do have dense cores.* × *50,000.*

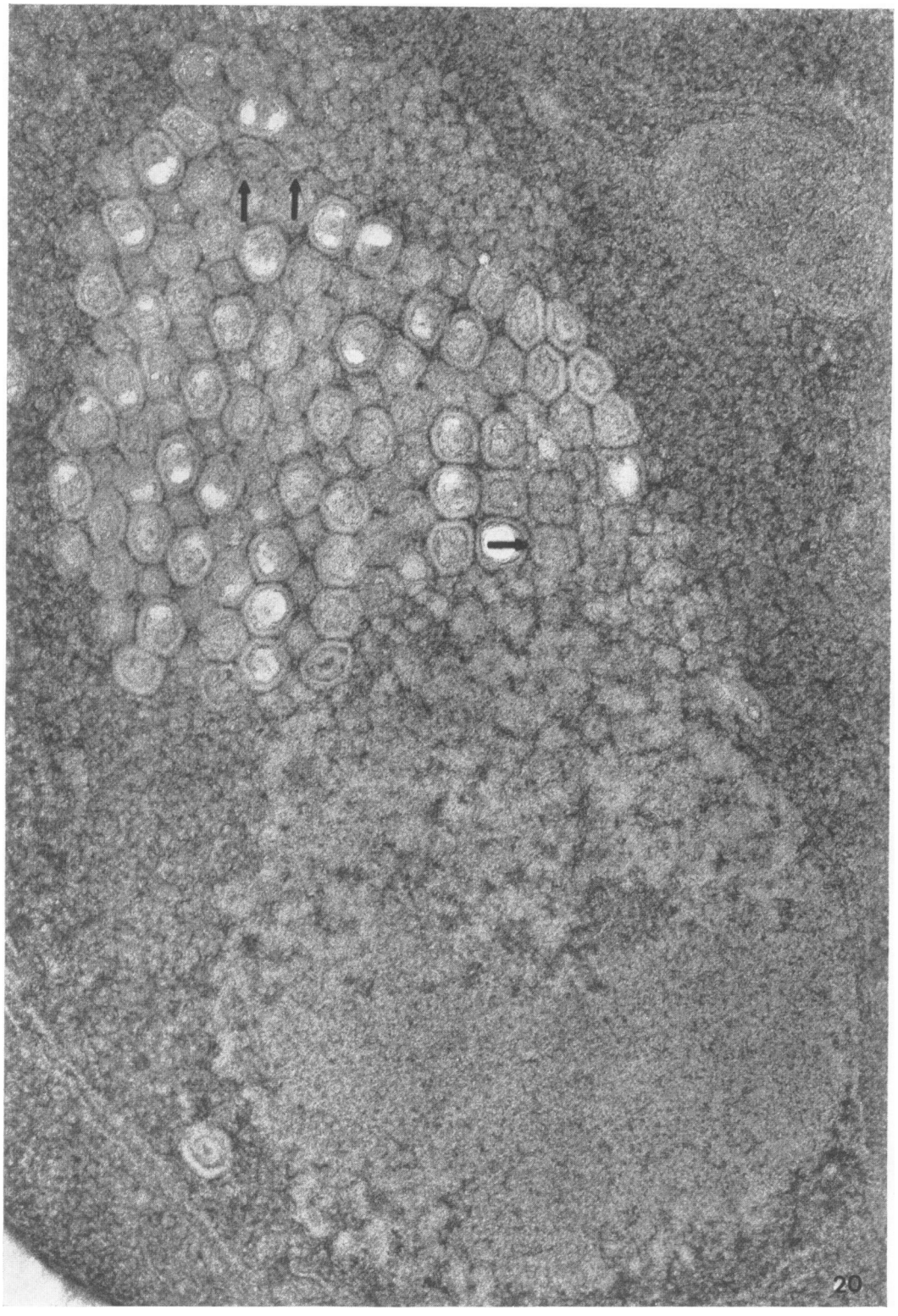

FIG. 20. *Nuclear complex consisting of a disintegrating round body, amorphous material, and a viral crystal. Small aggregates of granules are localized adjacent to the upper and lower right portions of the crystal where some capsids (arrows) are partially formed. Negatively stained sections.* × *75,000.*

to the upper and lower right portions of the viral crystal where several capsids (arrows) appear to be in the process of formation.

Figure 21 (usual sections) shows three aggregates of finely granular and fibrillar material (arrows) in the nucleus, which are apparently different in appearance from the granular aggregate described above. The aggregate at the center is localized adjacent to a collection of capsids, one of which facing the aggregate is partially formed. Such finely granular and fibrillar aggregates in the negatively stained sections are shown in Fig. 22 where the aggregates (arrows) accompanied with viral capsids are scattered in the nuclear matrix.

DISCUSSION

The cells for the negative staining of thin sections were prepared for electron microscopy in the same manner as those for the usual sections, except for drying of cells prior to embedding into epoxy resin. However, some cellular structures seen in both sections were different in appearance in the following points. First, ribosomes in the cytoplasm of uninfected cells were observed in the usual sections but were not discernible in the negatively stained sections. Similar observations were reported by Morris (10) with air-dried cysts of *Artemia salina* which were prepared for electron microscopy by totally anhydrous techniques. It is not unreasonable to assume that ribosomes may differ in affinity for heavy metals usually employed for thin sections so as to be distinguished from the cytoplasmic ground substance. However, visualization of cellular structures by negative staining may depend upon the penetrability of PTA into each cellular component. Second, no remarkable difference in appearance of the cytoplasmic ground substance was observed between uninfected and infected cells in the usual sections (cf. Fig. 1 and 3 with Fig. 6 and 9). In the negatively stained sections, however, the cytoplasmic ground substance of infected cells was apparently different in granularity from that of uninfected cells (cf. Fig. 7 and 10 with Fig. 2 and 4). The entire cytoplasmic ground substance of the infected cells has been replaced with granular material. Such material does not appear to be identical with ribosomes but may be products induced in cells by HSV infection since ribosomes seen in the usual sections do not appear to differ in distribution between uninfected and infected cells (cf. Fig. 1 and 3 with Fig. 6 and 9). This suggests that some fine structural alterations induced in cells can be revealed by the negative staining of thin sections but not by the usual sections. Third, nuclear aggregates of relatively uniform granules were observed in infected cells in both the usual and negatively stained sections. As noted in the insets of Fig. 15, the size of the granule was bigger in the negatively stained sections and the space between each granule was wider in the usual sections. However, the center-to-center distance between the granules appeared to be similar in both sections. This suggests that the negative staining of thin sections may reveal the entire surface of the granule, but the usual staining with heavy metals may be limited rather to the inner portion of the granule.

Previous studies of HSV-infected BHK-21 cells with ferritin-conjugated antibodies against HSV (7) have demonstrated that some viral antigens accumulate frequently in the cytoplasm near the cell membrane or near the nucleus. Such antigens were associated with material which resembles, with respect to their morphological appearance and their localization in the cytoplasm, the aggregates of granular and filamentous material observed in the present study (Fig. 9 and 10). The cytoplasmic granular material revealed in the negatively stained sections, as discussed above, may be associated with viral antigens since some cytoplasmic viral antigens were also demonstrated by ferritin-conjugated antibodies to be diffusely spread throughout the cytoplasm of HSV-infected BHK-21 (7) and HeLa (14) cells.

The present examinations of HSV-infected cells suggest the following sequence of events for formation of the viral core and capsid within the nucleus. Dense round bodies frequently appear in the nucleus near the nuclear membrane. Presumably, they are one of the early viral products induced by HSV infection, since similar dense bodies were reported previously to appear in the nucleus of HSV-infected BHK-21 cells before viral differentiation and to react with ferritin-conjugated antibodies specific for HSV (7). Subsequently, portions of the round body may be converted into another material which was observed as dense amorphous material. Such material, which also has viral antigenicity (14), appears to be closely related to formation of the granules of relatively uniform size and shape since the material was frequently localized in the area between the disintegrating round body and the granular aggregate (Fig. 12, 13, and 20). Granule formation may occur quickly and in an orderly manner to form aggregates consisting of rows of granules. Viral cores and capsids may be formed simultaneously within the aggregate in such a manner as to suggest that each granule represents a subunit and the several adjoining

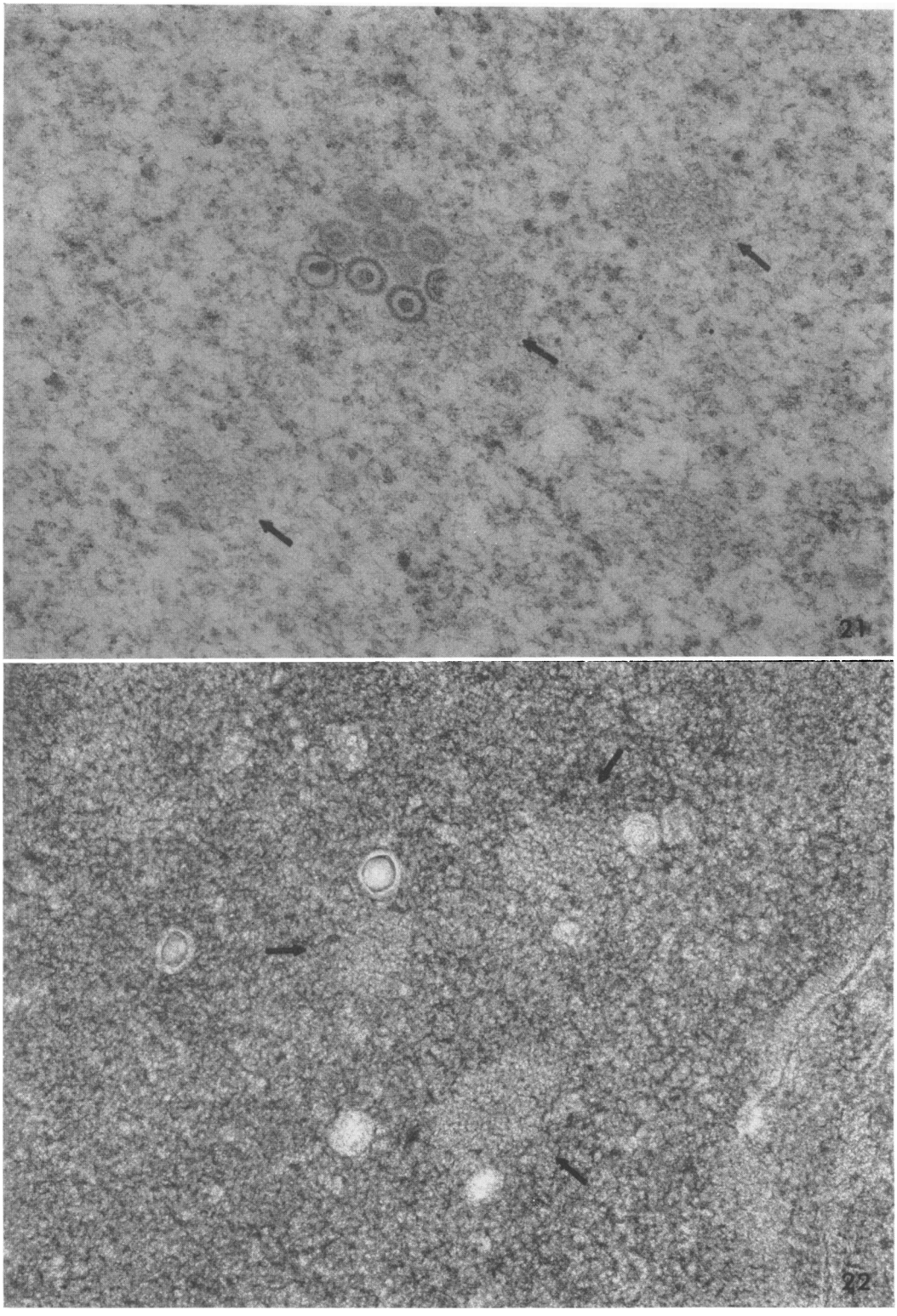

FIG. 21. *Three nuclear aggregates of finely granular and fibrillar material (arrows) and a collection of capsids with cores, one of which is partially formed. Usual sections.* × *62,500.*

FIG. 22. *Finely granular aggregates (arrows), similar to those in Fig. 21, associated with capsids with cores. Negatively stained sections.* × *62,500.*

subunits constitute the requirement for formation of a single capsid with a core. This concept is reinforced by the following three observations. First, some partially formed capsids enclose several (three to four) granules which themselves resemble in appearance the granules within the aggregate (Fig. 17). Second, the diameter of the granular core is approximately the same as the outside length of two adjoining granules within the aggregate (Fig. 17). Third, the capsid is big enough in diameter to enclose four granules arranged in rows in a square when measured in a plane of sections. These observations immediately suggest that a single capsid may enclose eight granules at most during its formation. Initially, the granules which become enclosed by the capsid would partially fuse with each other so as to form a core of doughnut shape (Fig. 13, 16–18) and, subsequently, the cores of low density would be formed. With HEp-2 cells infected with various strains of HSV, Schwartz and Roizman (19) reported the limited nuclear localization of capsids with electron-translucent cores, similar to those of doughnut shape in the present study. Neither the granules nor the cores at early stages of formation may contain enough viral deoxyribonucleic acid to show such an electron density as seen in the dense cores of enveloped particles (cf. Fig. 13 with Fig. 6). Rapid formation, orderly or randomly, of cores and capsids within the aggregate would replace the rows of granules with the rows of virus. It has been reported that core protein differs antigenically (7) and electrophoretically (16) from capsid protein. Thus, it may be concluded that the nuclear aggregate of uniform granules is the site where core and capsid proteins are differentiated and assembled into virus particles in the form of viral crystals, which were first reported by Morgan et al. (8).

As noted in Fig. 21 and 22, on the other hand, many capsids, some of which were apparently in the process of formation, were observed scattered throughout the nucleus without any relationship to the granular aggregate. However, such "scattered" capsids were frequently associated with small aggregates of finely granular and fibrillar material which were dispersed in the nucleus. Similar finely granular material was also observed in the nucleus of HSV-infected BHK-21 cells and was suggested to be closely related to capsid formation (7). Whether such finely granular material does originate from the round body remains undetermined.

The aggregates of uniform granules, similar to those discussed above, have been seen in nuclei of cells infected with most herpesviruses such as HSV (2, 9, 13, 19, 20, 23), feline herpesvirus (1), herpesvirus of turkeys (11), Marek's disease virus (3), and virus of frog adenocarcinoma (22), and their relationship to virus replication has been discussed for many years. The concept described above concerning the biological significance of the granules is not dissimilar in broad outline to that proposed in 1959 by Morgan et al. (9). In connection with the mechanism of viral crystallization, they have suggested in the studies of HSV-infected HeLa cells embedded in methacrylate that "the granular areas represent foci in which the various components of the viral particle become spatially arranged so as to present the electron microscopic appearance of a central body (core) and a single outer membrane (capsid)."

Morris (10) demonstrated the negatively contrasted cellular structures of cryptobiotic cysts of *artemia salina*, which were dried with phosphorous pentoxide in evacuated desiccators, and fixed in dry osmium tetroxide vapors, washed in ethylene glycol ether (17), embedded in epoxy resin, and stained with PTA. When HeLa cells prefixed with glutaraldehyde were dried with phosphorous pentoxide in the presence of osmium tetroxide vapors and then embedded in epoxy resin, the cellular structures showed negative contrast but were poorly preserved. However, the negatively contrasted and well-preserved structures were obtained when the cells were dried after usual fixation and dehydration. Thus, it is evident that drying of cells at any steps prior to embedding into epoxy resin results in the negative staining of thin sections with PTA. Such procedures would also prevent heavy metals, usually employed for thin sections, to bind some cellular structures (see Fig. 8). The mechanism whereby the thin sections of dried cells are stained negatively with PTA must be determined by further study.

The present observations indicate that the negative staining of thin sections would be an excellent tool to obtain detailed information concerning fine structural alterations induced in host cells by virus infection and to follow the mechanisms whereby viruses are formed. By the use of this technique, such cells infected with murine leukemia virus are currently under investigation where any specific structural alterations have not been detected by the usual sections, except for budding of the virus from the cell membrane.

ACKNOWLEDGMENTS

I thank Carol Owen and Mary Alice Burroughs for their excellent technical assistance and Berge Hampar for the use of his tissue culture facilities. I also thank Raymond V. Gilden, Flow

Laboratories, Inc., for the use of facilities during my stay as an exchange visitor.

LITERATURE CITED

1. Abraham, A., and P. Tegtmeyer. 1970. Morphological changes in productive and abortive infection by feline herpesvirus. J. Virol. 5:617–623.
2. Bedoya, V., A. S. Rabson, and P. M. Grimley. 1968. Growth in vitro of herpes simplex virus in human lymphoma cell lines. J. Nat. Cancer Inst. 41:635–652.
3. Epstein, M. A., B. G. Achong, A. E. Churchill, and P. M. Biggs. 1968. Structure and development of the herpes type virus of Marek's disease. J. Nat. Cancer Inst. 41:805–820.
4. Horne, R. W. 1967. Electron microscopy of isolated virus particles and their components, p. 521–574. *In* K. Maramorosch and H. Koprowski (ed.), Methods in virology, vol. III. Academic Press Inc., New York.
5. Hummeler, K., N. Tomassini, and B. Zajac. 1969. Early events in herpes simplex virus infection: a radioautographic study. J. Virol. 4:67–74.
6. Millonig, G. 1961. Advantages of a phosphate buffer for OsO_4 solutions in fixation. J. Appl. Phys. 32:1637.
7. Miyamoto, K., C. Morgan, K. C. Hsu, and B. Hampar. 1971. Differentiation by immunoferritin of herpes simplex virion antigens with the use of rabbit 7*S* and 19*S* antibodies from early (7-day) and late (7-week) immune sera. J. Nat. Cancer Inst. 46:629–646.
8. Morgan, C., E. P. Jones, M. Holden, and H. M. Rose. 1958. Intranuclear crystals of herpes simplex virus observed with the electron microscope. Virology 5:568–571.
9. Morgan, C., H. M. Rose, M. Holden, and E. P. Jones. 1959. Electron microscopic observations on the development of herpes simplex virus. J. Exp. Med. 110:643–656.
10. Morris, J. E. 1968. Dehydrated cysts of Artemia salina prepared for electron microscopy by totally anhydrous techniques. J. Ultrastruct. Res. 25:64–72.
11. Nazerian, K., L. F. Lee, R. L. Witter, and B. R. Burmester. 1971. Ultrastructural studies of a herpesvirus of turkeys antigenically related to Marek's disease virus. Virology 43:442–452.
12. Nii, S., and J. Kamahora. 1961. Cytopathic changes induced by herpes simplex virus. Biken. J. 4:51–58.
13. Nii, S., C. Morgan, and H. M. Rose. 1965. Electron microscopy of herpes simplex virus. II. Sequence of development. J. Virol. 2:517–536.
14. Nii, S., C. Morgan, H. M. Rose, and K. C. Hsu. 1968. Electron microscopy of herpes simplex virus. IV. Studies with ferritin-conjugated antibodies. J. Virol. 2:1172–1184.
15. Nii, S., H. S. Rosenkranz, C. Morgan, and H. M. Rose. 1968. Electron microscopy of herpes simplex virus. III. Effect of hydroxyurea. J. Virol. 2:1163–1171.
16. Olshevsky, U., and Y. Becker. 1970. Herpes simplex virus structural proteins. Virology 40:948–960.
17. Pease, D. C. 1966. The preservation of unfixed cytological detail by dehydration with "inert" agents. J. Ultrastruct. Res. 14:356–378.
18. Reynolds, E. S. 1963. The use of lead citrate at high *p*H as an electron-opaque stain in electron microscopy. J. Cell Biol. 17:208–212.
19. Schwartz, J., and B. Roizman. 1969. Similarities and differences in the development of laboratory strain and freshly isolated strains of herpes simplex virus in HEp-2 cells: electron microscopy. J. Virol. 4:879–889.
20. Siegert, R., and D. Falke. 1966. Elektronenmikroskopische Untersuchungen über die Entwicklung des Herpesvirus hominis in Kulturzellen. Arch. Gesamte Virusforsch. 19:230–249.
21. Sirtori, C., and M. Bosisio-Bestetti. 1967. Nucleolar changes in KB tumor cells infected with herpes simplex virus. Cancer Res. 27:367–376.
22. Stackpole, C. W. 1969. Herpes-type virus of the frog renal adenocarcinoma. I. Virus development in tumor transplants maintained at low temperature. J. Virol. 4:75–93.
23. Swanson, J. L., J. E. Craighead, and E. S. Reynolds. 1966. Electron microscopic observations on herpesvirus hominis (herpes simplex virus) encephalitis in man. Lab. Invest. 15:1966–1981.